Determination of the differential cross section for a realistic intermolecular potential

Andrzej Herczyński
American Institute of Physics, One Physics Ellipse, College Park, Maryland 20740-3843

Ryszard Herczyński and Artur Kozłowski
Institute of Fundamental Technological Research, Polish Academy of Sciences, ulica Swietokrzyska 21, 00-226 Warszawa, Poland
(Received 23 December 1993)

A method for obtaining the differential cross section for any realistic intermolecular potential (e.g., the Lennard-Jones potential), is presented. This approach avoids *ad hoc* approximations, such as the finite-range potentials and angular cutoffs, and can be used for accurate calculations of the transport coefficients. It is shown that neither the hard spheres nor the soft spheres (variable hard spheres) models are consistent with a realistic potential, even in the limit of large relative molecular velocity.

PACS number(s): 05.20.Dd, 51.10.+y, 34.20.Cf

I. INTRODUCTION

In abbreviated form, the Boltzmann equation for a monatomic gas without internal degrees of freedom can be written as

$$\frac{Df}{Dt}=I(f,f)\ , \tag{1}$$

where $Df/Dt=\partial f/\partial t+\mathbf{c}\partial f/\partial \mathbf{x}$, and $I(f,f)$ denotes the collision integral. Mass forces have been omitted. Here as usually $\mathbf{c}$ is the molecular velocity, $\mathbf{x}$ and t are space and time coordinates, respectively, and f denotes the probability distribution function. Characters in bold fonts represent vectors.

The collision integral can be represented in two, not entirely equivalent, forms. The stochastic form reads

$$I(f,f)=-\int_C\int_0^{2\pi}\int_1^{-1}[f(\mathbf{c}')f(\mathbf{c}_*')-f(\mathbf{c})f(\mathbf{c}_*)]\times w(s,g^2)g\,ds\,d\phi\,d\mathbf{c}_*\ , \tag{2}$$

whereas the deterministic form is

$$I(f,f)=\int_C\int_0^{2\pi}\int_0^{\infty}[f(\mathbf{c}')f(\mathbf{c}_*')-f(\mathbf{c})f(\mathbf{c}_*)]\times bg\,db\,d\phi\,d\mathbf{c}_*\ . \tag{3}$$

In both (2) and (3), $\mathbf{c}$ and $\mathbf{c}_*$ denote velocities of colliding molecules before the collision, and $\mathbf{c}'$ and $\mathbf{c}_*'$ velocities after the collision, $g=|\mathbf{c}_*-\mathbf{c}|=|\mathbf{c}_*'-\mathbf{c}'|$ is the absolute value of the relative velocity, ϕ is the azimuthal angle, and the distribution function is also implicitly dependent on $\mathbf{x}$ and t.

In the stochastic form, $w(s,g^2)$ denotes the density of probability that the cosine of the deflection angle χ after the collision of two molecules having relative speed g will be equal to s, $s=\cos\chi$. The function $w(s,g^2)$ is related to the differential cross section $\sigma=\sigma(\chi,g^2)$ by

$$w(s,g^2)ds=-\sigma(\chi,g^2)\sin\chi\,d\chi\ . \tag{4}$$

In the deterministic form of the collision integral, b denotes the impact parameter. The main difference between (2) and (3) arises from the fact that whereas in the stochastic form the integration is carried over an "after-the-collision" parameter s, in the deterministic form the integration is performed over a "before-the-collision" parameter b.

For any given value of b and any spherically symmetric intermolecular potential $\Phi,\Phi=\Phi(r)$, the deflection angle χ can be calculated in the frames of classical mechanics from the set of equations based on the first principles (e.g., [1], Chap. 1). Thus for a given potential one can always find [see (A1) in Appendix A]

$$s=s(b,g^2)=\cos\chi(b,g^2)\ . \tag{5}$$

Almost all actually performed calculations for the full Boltzmann equation employ the Monte Carlo computational method and are based on the deterministic form of the Boltzmann equation. In the majority of these calculations it is assumed also that molecules are elastic spheres, $\sigma=$const, i.e., the hard spheres potential is used. Less often, the soft spheres [or variable hard spheres (VHS)] potential is employed, for which $\sigma=\sigma(g^2)$, [2], or its generalizations such as the generalized hard spheres (GHS) [3] and the optimal VHS [4].

The main obstacle to using the stochastic form of the Boltzmann equation is the difficulty of determining the differential cross section $\sigma(\theta,g^2)$, or, alternatively, $w(s,g^2)$, for a realistic intermolecular potential. Once the differential cross section is known, however, evaluating the collision integral in the stochastic form (2) is much easier than using the deterministic form (3). In the latter case, one needs to calculate the deflection angle χ for each value of the impact parameter b in order to find $\mathbf{c}'$ and $\mathbf{c}_*'$, the step which is not necessary if (2) is used.

The aim of this paper is to describe a method of finding $w(s,g^2)$ for an arbitrary intermolecular potential (the salient idea of the method was briefly introduced in [5]). Along the way, it is pointed out that neither the hard spheres nor soft spheres potential represents a proper limit of a realistic potential for collisions with relatively high energy, as is commonly believed. Therefore, the va-

lidity of the quantitative results obtained using these approaches remains suspect even in this limit.

II. NONMONOTONIC POTENTIALS

If the intermolecular potential $\Phi=\Phi(r)$ is monotonic, the function inverse to $s=s(b,g^2)$ in (5), $b=b(s,g^2)$, exists, and hence $w(s,g^2)$ can be expressed by

$$w(s,g^2)=\frac{1}{2}\left|\frac{\partial b^2}{\partial s}\right| . \tag{6}$$

However, in the case of a nonmonotonic intermolecular potential Φ, the function $s=s(b,g^2)$ is nonmonotonic also, and (6) ceases to be meaningful. Since all realistic intermolecular potentials are nonmonotonic, (6) is of no help in practical applications to real systems, and an alternative approach must be developed.

Although the method presented here is not restricted to any particular form of the potential, it is best to illustrate it with a specific intermolecular force in mind. In what follows, the most common realistic potential, the Lennard-Jones potential, is assumed. In the standard nondimensional form, the 6-12 Lennard-Jones potential is represented as

$$\Phi(r)=4(r^{-12}-r^{-6}) , \tag{7}$$

where $\Phi(r)=\Phi'(r'/\sigma_0')/\varepsilon'$ and the dimensional quantities are denoted by primes. Here, ε' and σ_0' represent the reference energy and the reference length characteristic for the potential under consideration. In the remainder of this paper, all variables without primes are nondimensional. They are defined via the following: $r=r'/\sigma_0'$ (and $b=b'/\sigma_0'$), $T=k'T'/\varepsilon'$, and $g^2=m'g'^2/2\varepsilon'$, where m' is the molecular mass. Equations (1)–(6) can be considered as nondimensional, and therefore the lack of primes in them (except those denoting velocities after the collision) does not lead to inconsistencies.

Once the potential has been selected, the dependence of the deflection angle χ, or s, on the impact parameter b (with the relative velocity of the molecules g as a parameter) can be examined. Graphs of the function $s=s(b,g^2)$ for the Lennard-Jones potential (7) are shown in Fig. 1. (Similar graphs are given in [1], Fig. 120). These graphs, as expected, are nonmonotonic, and therefore, again, the inverse of s is not a well defined function.

On the other hand, (6) indicates that even when the function $b=b(s,g^2)$ could be extracted, it would contain more information than is actually needed to obtain $w(s,g^2)$, which is a probability density. This suggests that one encodes the useful information contained in the graphs of Fig. 1 by means of the integral quantity

$$W(s,g^2)=\int_0^{1-s} b^2(u,g^2)du . \tag{8}$$

It should be noted that even though W does contain information about the inverse of s, it is always a well defined monotonic function, no matter whether $s(b,g^2)$ is monotonic or not (see Appendix B). In effect, it is a sum of the probability densities for deflection through angles smaller than a given angle. Once W is known, the function $w(s,g)$ can be found by setting

$$w(s,g^2)=-\frac{1}{2}\frac{\partial^2 W}{\partial s^2} . \tag{9}$$

In the case of monotonic potential, this relation is equivalent to (6). The point of the method is, however, that W can be obtained in fact without the knowledge of $b=b(s,g^2)$ by numerical integration of the known function $s=s(b,g^2)$ "inverse" to $b(s,g^2)$.

III. THE DIFFERENTIAL CROSS SECTION

When the Lennard-Jones potential (7) is used, the numerical integration of (8) is easily performed for the case $g^2>1$. For $g^2<1$, the function $S(b,g^2)=1-s(b,g^2)$ exhibits rapid oscillations after the initial monotonic decline from 1 at $b^2=0$ to 0 at $b^2<2$; see Figs. 1(a) and 1(b). These oscillations, which grow in number when the value of g decreases, correspond to the "trapping" effect. By trapping one understands a collision in which the incoming particle (in the coordinate system attached to the other one) is captured for a while and spins around the "stationary" molecule. These loops are sometimes called "Glory orbits" (for a classical treatment see, e.g., [6]; for a semiclassical analysis see [7]). Although the number of Glory orbits is always finite, it is not bounded as g decreases. One could in principle compute the integral in (8) taking into account all the oscillatory behavior of the function $S(b,g)$ for $g^2<1$. However, this is not necessary.

This paper deals with the physical conditions for which a gas can be described by the Boltzmann equation (1) with (2), taking into account only binary collisions. It is assumed that the gas is warm, with the temperature well above 0 K. In a real system under such conditions, trapping is extremely unlikely to occur, and a configuration of two spinning molecules produced by a collision is unstable. Further, it is safe to assume that when a spinning pair breaks apart, all scattering angles are equally probable and hence the overall probability of scattering through a given angle is not affected. Thus trapping can be considered as a mathematical artifact of analyzing one collision at a time, and there is no need to include all details of the "comb" in Figs. 1(a) and 1(b) when performing integration (8).

For similar reasons, one can limit the domain of g from below, keeping in mind that g is a magnitude of the relative velocity of the particles when they are infinitely far apart. On physical grounds, therefore, one can exclude from considerations the region of very small g ($g \ll 1$). The magnitude of this region depends on the temperature of the gas and grows when the temperature increases.

In the evaluation of integral (8) employed here, oscillations in $s(b,g^2)$ were replaced by a straight line joining the second local minimum of the function with the last local maximum. Figure 2 shows the function $W(s,g^2)$ for several values of g^2. It is important to note that the curves in Fig. 2 are not parabolic. They are steeper near $s=1$ than the best fitting parabolas. Since the second derivative of W (or curvature) is of physical interest, the analytic approximation of W should be very accurate, for

example using the method of splines. For illustrative purposes, however, a less accurate approximation is chosen here, leading to the function w in a simple, polynomial form. This approach also makes the physical interpretation of the resultant expression for w easier.

The function W is thus approximated for each g^2 by a polynomial in s by means of the least square method, requiring $W_{\text{app}}(1,g^2)=0$ for all g^2. In trying these approximations, it is easily seen that polynomials of the second and third order do not give satisfactory results but the approximation of the fourth order is accurate to less than 1%. Only for large values of g^2 ($g^2>10$), and in the region close to $s=1$, the fourth order approximation is not very accurate. This is due to the presence of a flat hump seen in Fig. 1(f). The use of still higher order polynomials does not substantially change the accuracy of the approximation, and leads to undesirable wiggles superimposed on the curves. Thus it is useful to set

$$W(s,g^2)=\sum_{i=0}^{4} a_i(g^2)s^i , \tag{10}$$

where $a_i(g^2)$ are coefficients computed separately for each g^2. The coefficients a_0 and a_1 in expansion (10) are of no consequence so far as the calculations of the stochastic function $w(s,g^2)$ are concerned. The other three coefficients $a_2(g^2)$, $a_3(g^2)$, and $a_4(g^2)$ are plotted in Figs. 3(a)–3(c). It is seen that these functions are not monotonic with respect to g^2: they all have a local maximum near $g^2=1$, fall down to a local minimum, rise steeply

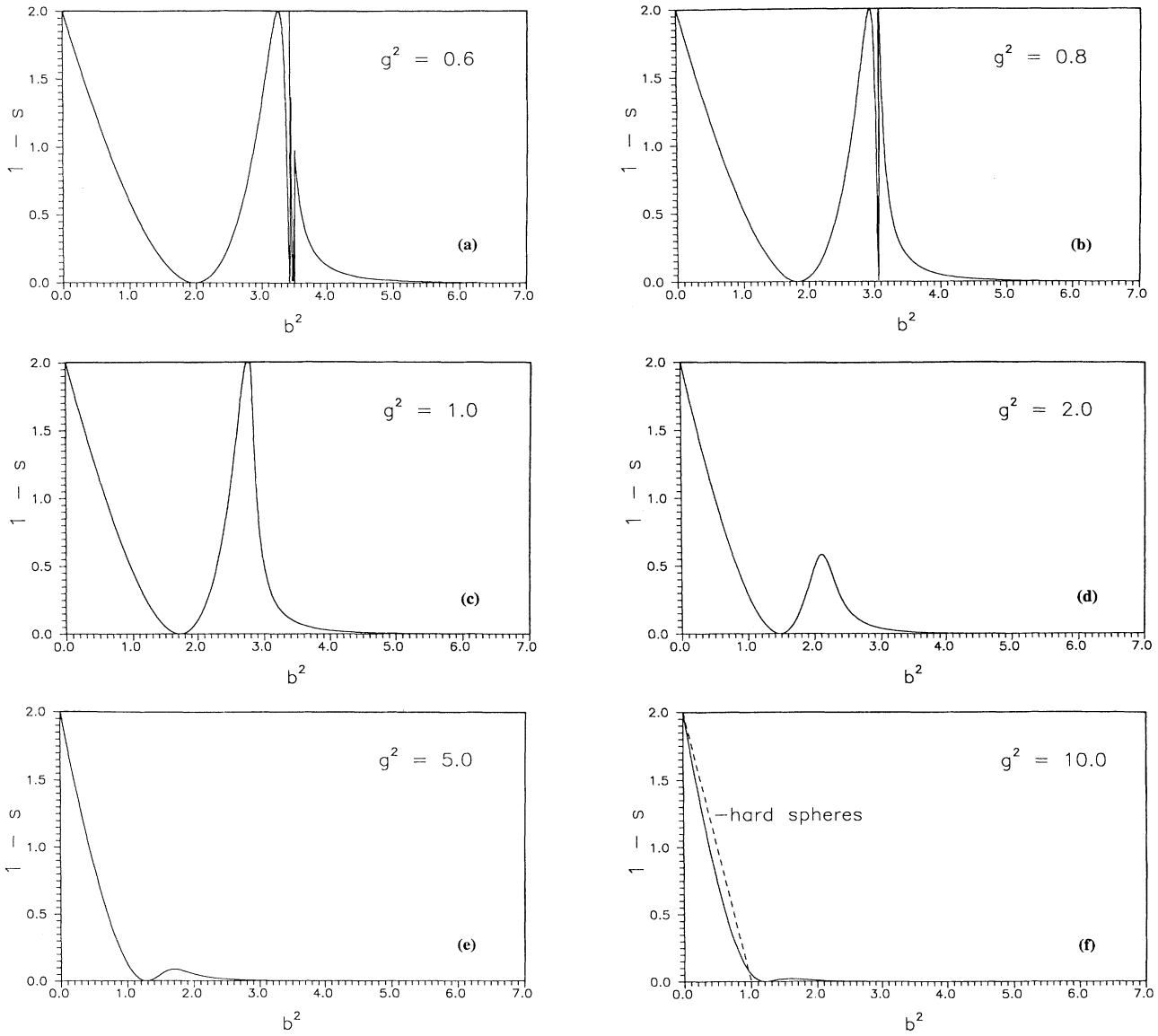

FIG. 1. Deflection $1-s$ as a function of the impact parameter for the Lennard-Jones potential, for several values of the relative molecular velocity g^2. (a) $g^2=0.6$. (b) $g^2=0.8$. (c) $g^2=1.0$. (d) $g^2=2.0$. (e) $g^2=5.0$. (f) $g^2=10.0$. The dashed line represents the deflection for the hard spheres potential. All variables, in these and the following graphs, are normalized.

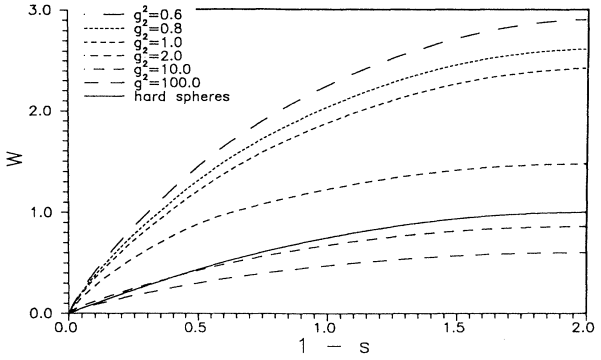

FIG. 2. The function W plotted vs $1-s$ for several values of the relative molecular velocity g^2. The continuous line represents the result for the hard spheres potential.

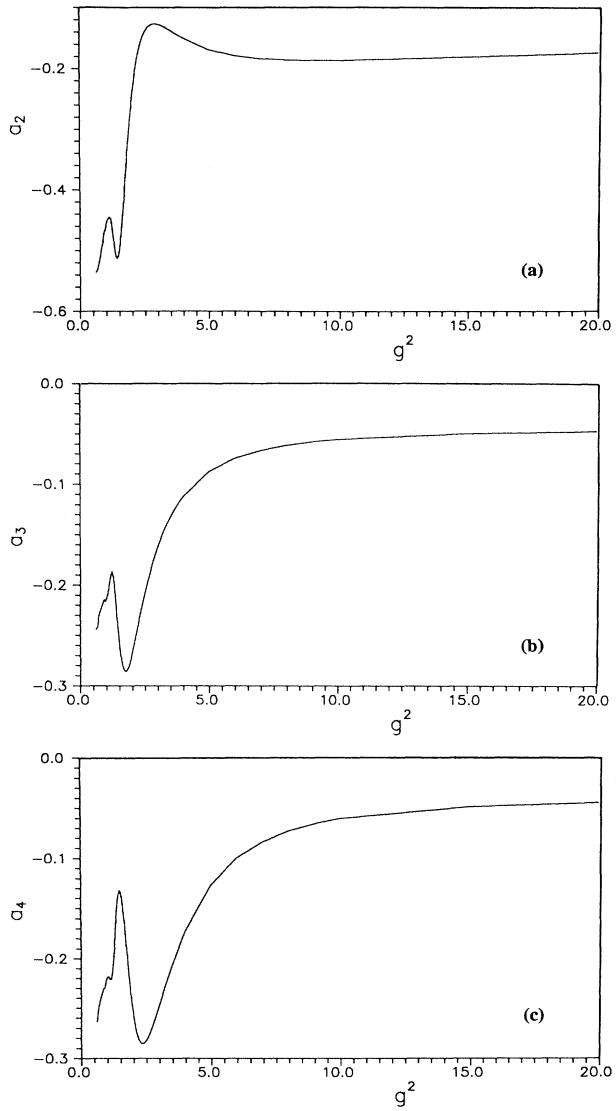

FIG. 3. Coefficients of the fourth order polynomial approximation of W plotted vs the relative molecular velocity g^2. (a) Coefficient a_2. (b) Coefficient a_3. (c) Coefficient a_4.

near $g^2=2$, and then level off. This behavior near $g^2=1$ is due to the qualitative transition in scattering curves seen at this value of g^2 in Fig. 1(c).

Bypassing the details of Glory orbits (or the trapping effect) is not central to the proposed method and is only a matter of convenience, simplifying calculations. All the steps outlined here can be repeated replacing the presented evaluation of integral (8) with a numerical method of one's choice. On the other hand, since the oscillations corresponding to Glory orbits, such as those shown in Figs. 1(a)–1(c), are symmetrical with respect to $s=0$ and are localized over a small range of values of b^2, the numerical effect of neglecting them is marginal. Whether these loops are included or not, the physics of the realistic intermolecular potential, including its attractive part, is fully retained.

To further emphasize this point, it is instructive to repeat the calculations for a potential that does not include the attractive part of the Lennard-Jones interaction, taking, for example, the potential given by $\Phi=4r^{-1/2}$ in a normalized form. As expected, the resulting functions $s(b,g^2)$, with b treated as a parameter, are monotonic (Fig. 4). The corresponding functions W can now be obtained equally easily as before, and one can show that all coefficients $a_i(g^2)$ entering approximations of these functions are strictly monotonic. In fact, a_3 and a_4 turn out to be almost constant for this case.

It follows from (9) that the stochastic function w (the differential cross section) is given by

$$w(s,g^2)=-a_2(g^2)-3a_3(g^2)s-6a_4(g^2)s^2 . \qquad (11)$$

Figure 5 contains plots of w for several values of g^2, for both the full Lennard-Jones potential and for the hard spheres potential. For hard spheres, the function w is constant and equal to $\frac{1}{4}$, as can be seen immediately from (6) since in this case $b=\sin\theta$ or $b^2=(s+1)/2$ (the radius of the billiard balls has been normalized to 1). For the Lennard-Jones potential, $w(s,g^2)$ is a family of parabolas with (nonmonotonic) coefficients dependent on g^2; their minima occur near $s=-0.25$ or $\theta\simeq 104°$. It can be seen from Fig. 5 that as g^2 increases, the differential cross section corresponding to the Lennard-Jones potential does

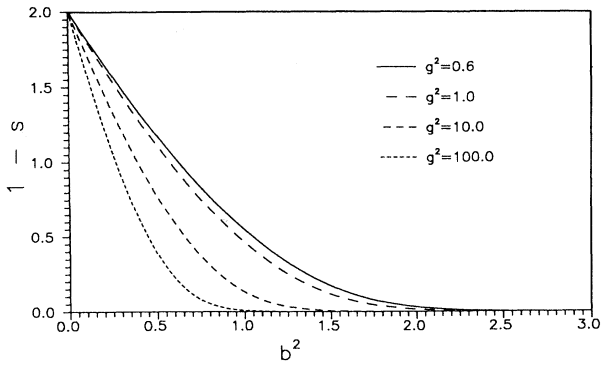

FIG. 4. Deflection $1-s$ as a function of the impact parameter b^2 for several values of the relative molecular velocity g^2, for the repulsive part of the Lennard-Jones potential.

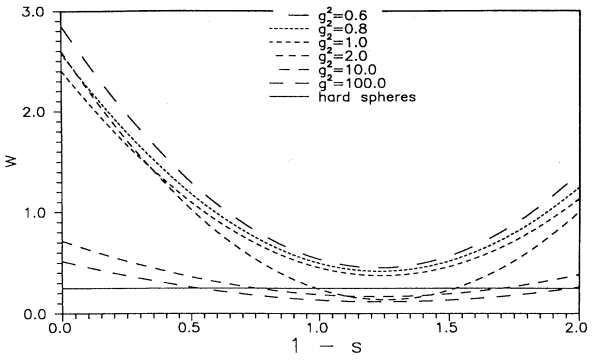

FIG. 5. Scattering function w [related to the differential cross-section via (4)] vs $1-s$ for several values of the relative molecular velocity g^2. The continuous line represents the hard spheres potential.

not tend to the hard spheres differential cross section. For small relative velocities ($g^2 < 10$), on the other hand, hard spheres is a demonstrably inadequate approximation of a realistic intermolecular potential.

IV. CHAPMAN-COWLING INTEGRALS

To illustrate how the present approach may be used for accurate calculation of the transport coefficients, the Chapman-Cowling integrals Q^1, Q^2, and Q^4 are evaluated in this section. In the current notation, these functions are defined (compare [1], Eq. 8.2-3) as

$$Q^l(g)=\frac{4(1+l)}{(-1)^l-2l-1}\int_{-1}^{1}(1-s^l)w(s,g^2)ds \ . \qquad (12)$$

Integrals Q^l have been normalized with respect to the hard spheres potential. They are the same as the Chapman-Cowling functions $\phi^l(g)$ divided by g and multiplied by the factor in front of the integral in (12).

Once the functions Q^l are known, transport coefficients can be calculated easily according to the approximation scheme of Chapman and Cowling [8]. For example, the first approximations to the coefficients of self-diffusion D', viscosity η', and thermal conductivity λ' are conveniently given (in dimensional form) by

$$D'=\frac{3\sqrt{\pi m'k'T'}}{8\rho'\pi\sigma_0'^2\Omega^1}, \quad \eta'=\frac{5\sqrt{\pi m'k'T'}}{16\pi\sigma_0'^2\Omega^2}, \qquad (13)$$
$$\lambda'=c_v'\frac{25\sqrt{\pi m'k'T'}}{32\pi\sigma_0'^2 m'\Omega^2} \ ,$$

where m' is the molecular mass, k' is the Boltzmann constant, T' is the temperature, ρ' is the density, c_v' is the specific heat at constant volume, and

$$\Omega^l(T)=\frac{2}{(l+1)!}\int_0^\infty e^{-\gamma^2}\gamma^{2l+3}Q^l(g)d\gamma \ , \qquad (14)$$

with $\gamma^2=m'g'^2/2k'T'$.

Figure 6 is a plot of Q^1, Q^2, and Q^4 versus g^2 obtained from (12). As an alternative approach, one can sidestep approximation (10) and compute the second derivative of W directly, i.e., numerically. Figure 7 shows the

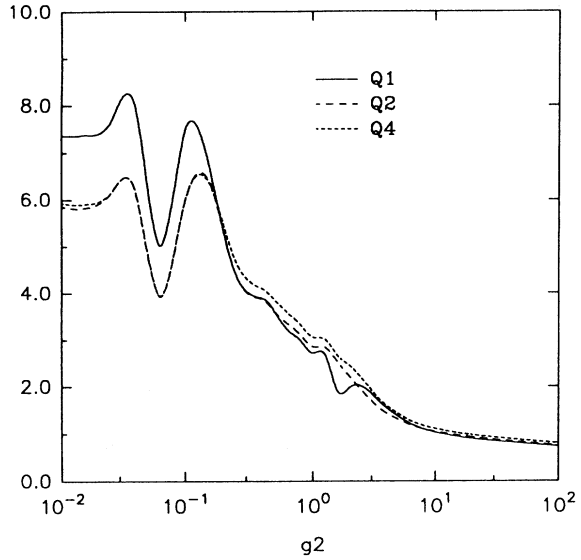

FIG. 6. The Chapman-Cowling integrals Q^1, Q^2, and Q^4 as functions of g^2, computed via approximation (11).

Chapman-Cowling integrals when this "direct" calculation of w is used in (12) instead of approximation (11). For $g^2 > 0.2$, functions Q^2 and Q^4 in Figs. 6 and 7 are in very good agreement with the values computed via a different method by Hirschfelder, Curtis, and Bird in [1] (Fig. 121). For Q^1, the "direct" method is in excellent agreement with Hirschfelder, Curtis, and Bird, whereas approximation (11) leads to a more pronounced hump near $g^2=1$ in Fig. 6. It should be noted again that, using a sufficiently accurate approximation of W, the Chapman-Cowling integrals can be computed with arbitrary precision.

An interesting feature of the calculated functions Q^l is

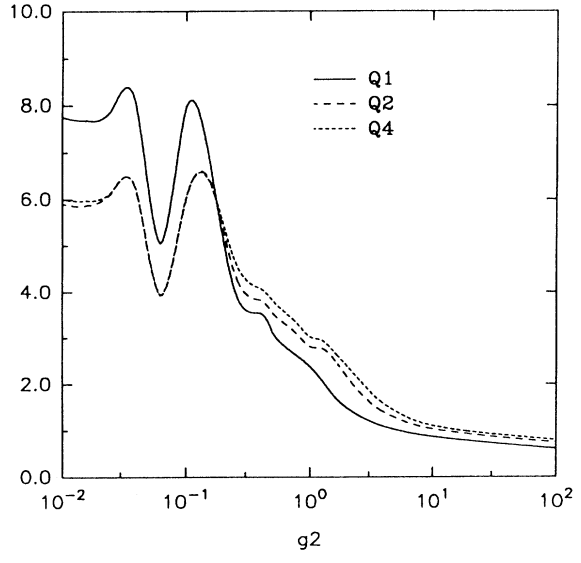

FIG. 7. The Chapman-Cowling integrals Q^1, Q^2, and Q^4 as functions of g^2, computed by the "direct" method.

their behavior for $g^2<0.1$, which, to the author's knowledge, has never been evaluated before (Hirschfelder's calculations for $0.1<g^2<0.2$ are also suspect). With the present method, the Chapman-Cowling integrals can be obtained for their entire domain. However, the values of these functions on the disputed interval $0<g^2<0.1$ will have negligible effect on integral (14), and therefore on transport coefficients (13).

V. CONCLUDING REMARKS

The approximation defined by (10) requires several additional comments. From (6) it follows that the integral

$$\int_{\pi}^{0}\sigma(\chi,g^2)\sin\chi\, d\chi=-\int_{-1}^{1}w(s,g^2)ds=\int_{0}^{\infty}b\, db\ , \qquad (15)$$

expressing the total effective cross section, diverges. Mathematically, this is due to the behavior of function $w(s,g^2)$ close to $s=1$ [or the behavior of $\sigma(\chi,g^2)$ close to $\chi=0$]. The physical reason for this divergence is the infinite range of the intermolecular potential. A collision of two molecules that are far apart changes only slightly their trajectories. More precisely, the deflection angle χ is $O(b^{-6})$ for the Lennard-Jones potential, or $O(b^{-n})$ for a potential in the form $\Phi(r)\cong r^{-n}, n>2$ (see Appendix A). These "grazing collisions" are responsible for the rise of σ close to $\chi=0$. (Considered in the frame of quantum theory, grazing trajectories are not well defined.)

To avoid the divergence mentioned above, it is sometimes assumed that the intermolecular potential acts only at a finite, specified range. A more frequent approach is to limit the integration over χ in the left-hand side of (15) to angles greater than some small $\chi_0>0$. In either of these two approaches, an arbitrary parameter is introduced and it determines to some extent the end results. The polynomial approximations (10) of W lead to a finite value of $w(s,g^2)$ at $s=1$, and therefore automatically avoid the difficulty of grazing collisions. Since these approximations are based on the behavior of W in the entire domain on which it is defined (i.e., $-1\le s\le 1$), the arbitrariness of the finite-range potentials or the cutoff angles is avoided. Only the accuracy of the approximate method described here remains arbitrary, and it can be chosen at will.

The problem of the divergence in (15) casts some doubt on the outlined procedure of determining the function W, and it should be carefully verified that the integral in (8) in fact converges. The proof of this is given in Appendix B.

It was already remarked in discussing Fig. 5 that, for the Lennard-Jones potential, the molecules do not become hard spheres in the limit of $g^2\to\infty$. This can be deduced already from Fig. 1(f). It is seen there that as the values of g^2 increase, the plot of $S(b,g^2)=1-s^2$ does not tend to the hard spheres limit shown by the dashed line in the figure. The graph for hard spheres has a finite discontinuity in the derivative at $b=1$, whereas the derivative of $S(b,g^2)$ is always finite and equal to 0 at the first minimum approaching $b=0$. The consequence of this fact is shown also in Fig. 2, where the graph corresponding to the hard spheres potential is also indicated.

One final point should be made. It was noted earlier that a polynomial approximation of the function W required, for consistency, polynomials of at least fourth order. It is significant that the second order approximation in (10) would have been insufficient. Such an approximation would imply that the resulting function $w(s,g^2)$, as given in (9), would depend only on g^2 and not on s, as is the case for the soft spheres. Indeed, the essence of the soft spheres approximation is that scattering through any angle is equally probable, and the effective cross section depends only on g^2. Equation (11) indicates, however, that the cross section must in fact depend on s. Thus it is shown that the VHS approximation is inconsistent with the use of a realistic intermolecular potential.

ACKNOWLEDGMENT

The authors thank Dr. Jan Herczyński for help in formulating Appendix A.

APPENDIX A

This appendix serves to derive an estimate of the deflection angle χ in the limit of $b\to\infty$; that is, for grazing collisions. It is assumed that the intermolecular potential has the most common form $\Phi(r)\cong r^{-n}, n>2$.

The deflection angle is given by the classical formula (e.g., [1], Eq. 5.26)

$$\chi(b,g^2)=\pi-2b\int_{r_m}^{\infty}r^{-2}h^{-1/2}(r)dr\ , \qquad (A1)$$

where $h(r)=1+ar^{-n}-b^2r^{-2}$, and where the energy of the molecule pair is assumed fixed. Here r_m represents the root of $h(r)=0$, and a is a constant dependent on the relative kinetic energy of the two molecules.

For a purely repulsive potential, $a<0$. In the case of the Lennard-Jones potential, the repulsive part can be ignored in the limit of large b and therefore $a>0$ can be assumed. Both cases will be considered, however.

The derivative of $h(r)$ is

$$\frac{dh}{dr}=-\frac{na}{r^{n+1}}+\frac{2b^2}{r^3}=-\frac{2b^2}{r^3}\left[\frac{na}{2b^2}\frac{1}{r^{n-2}}-1\right]\ . \qquad (A2)$$

If $a>0$, $h(0)=\infty$, $h(\infty)=1$, and the function has one extremum (minimum). At any point $r^*\in(0,\infty)$ one can find b large enough so that $h(r^*)<0$. Thus for each value of b there are two roots of the equation $h(r)=0$. Only the larger of the two roots is of interest, since only for it the function h remains positive in the limits of integral (A1). This root is denoted $r_m=r_m(b)$.

For $a<0$, $h(0)=-\infty$, $h(\infty)=1$, and $h'(r)>0$. In this case there exists only one root of the equation $h(r)=0$, and it is denoted again by r_m.

In both cases, for any given value $r=r_0$ there exists a value of b, say b_0, such that $r_m(b)>r_0$ for all $b>b_0$. In other words,

$$\lim_{b\to\infty}r_m(b)=\infty\ . \qquad (A3)$$

From the expression for $h(r)$, and the definition of r_m, it follows that

$$\frac{b^2}{r_m^2(b)}=1+\frac{a}{r_m^n(b)} \qquad (A4)$$

and hence, from (A3),

$$\lim_{b\to\infty}\frac{r_m(b)}{b}=1\ . \tag{A5}$$

Relation (A5) can be used to obtain a more accurate estimate of $b/r_m(b)$. Solving (A4) for a, and then using (A5), yields

$$\frac{b}{r_m(b)}=1+\frac{a}{2b^n}+O\left[\frac{1}{b^{n+1}}\right]\ . \tag{A6}$$

Now, by setting $r=tr_m$, the integral in expression (A1) can be rewritten

$$I_1=\frac{1}{r_m}\int_1^\infty t^{-2}\left[1+\frac{a}{r_m^n t^n}-\frac{b^2}{r_m^2 t^2}\right]^{-1/2}dt\ . \tag{A7}$$

Therefore, using (A6), in the limit of $b\to\infty$,

$$bI_1\to\int_1^\infty\frac{dt}{t^2(1-t^{-2})^{1/2}}=\frac{\pi}{2} \tag{A8}$$

and, from (A1),

$$\lim_{b\to\infty}\chi(b,g^2)=0\ . \tag{A9}$$

Equation (A9) is expected on physical grounds. A more precise estimate of χ can be obtained by observing that $h(r)=1-t^{-2}+O(b^{-n})$ for $b\to\infty$ and $r=tr_m$, uniformly on the interval $1\le t\le\infty$. Thus also

$$h^{-1/2}(r)=(1-t^{-2})^{-1/2}+O(b^{-n})\ , \tag{A10}$$

uniformly for t. Comparing with (A8), one obtains finally

$$\chi(b,g^2)=O(b^{-n}) \tag{A11}$$

for grazing collisions.

APPENDIX B

It will be shown here that the integral defined in (8) is uniformly convergent provided $\Phi(r)$ decreases fast enough. The proof will be given, again, for a potential in the form $\Phi(r)\cong r^{-n}$, $n>2$.

Estimate (A11) allows one to show that for any $B>0$ the integral

$$I_2=\int_B^\infty S(b,g^2)db^2 \tag{B1}$$

is uniformly convergent in the upper limit, that is to say, the integration over the "tail" in Figs. 1(a)–1(f) does not lead to infinities. To this goal, it is sufficient to note that

$$S(b,g^2)=1-\cos\chi(b,g^2)=O(b^{-2n})\ , \tag{B2}$$

where the cosine was expanded in the power series and (A11) was used. It therefore follows that $I_2<\infty$. Now let

$$I_3=\int_0^{S_0}b^2(s,g^2)ds\ . \tag{B3}$$

For any S_0 large enough so that b^2 is monotonic on the interval $(0,S_0)$, there exists a B_0 such that $S(B_0,g^2)=S_0$. Since $S(\infty,g^2)=0$, or $b^2(0,g^2)=\infty$, it follows from general properties of the definite integrals that with $B=B_0$, $I_3=I_2<\infty$. In other words, integral (8) is uniformly convergent.

[1] J. O. Hirschfelder, Ch. F. Curtis, and R. B. Bird, *Molecular Theory of Gases and Liquids* (Wiley, New York, 1954).
[2] G. A. Bird, in *Rarefied Gas Dynamics,* edited by S. S. Fisher (AIAA, New York, 1981), p. 239.
[3] H. A. Hassan and D. B. Hash, Phys. Fluids A **5**, 738 (1993).
[4] D. A. Erwin, Bull. Am. Phys. Soc. **34**, 2298 (1989).
[5] R. Herczyński and A. Herczyński, in *Current Topics in Shock Waves,* edited by Y. Kim, AIP Conf. Proc. No. 208 (AIP, New York, 1990), pp. 131–136.
[6] R. Newton, *Scattering Theory of Particles and Waves* (Springer-Verlag, New York, 1982).
[7] K. W. Ford and J. A. Wheeler, Ann. Phys. **7**, 259 (1959).
[8] S. Chapman and T. G. Cowling, *The Mathematical Theory of Non-Uniform Gases* (Cambridge University Press, Cambridge, 1939).